Original Research Paper   https://doi.org/10.46488/NEPT.2022.v21i04.003   **Open Access Journal**

Analysis of Alkali-Induced Soil Heaving in Non-Expansive Soil Using Electrokinetic Model

Manish Kumar Mandal* and Bala Ramudu Paramkusam*†

*Department of Civil Engineering, Indian Institute of Technology (Banaras Hindu University), Varanasi, India

†Corresponding author: Bala Ramudu Paramkusam; pbramudu.civ@itbhu.ac.in

ABSTRACT

An attempt has been made in this paper to conduct an Electrokinetic (EK) enhanced large-scale model study to analyze the heaving phenomena observed in fields. The application of the EK technique on fields to study alkali-induced heaving has been simulated in the laboratory using a rectangular and circular model. The EK technique was mainly employed to facilitate alkali soil interaction. Analysis of the geometry of the model boundary on the various physiochemical as well as geotechnical properties of the soil was conducted. Before that, a simple heaving analysis was also performed in an oedometer without the EK technique. Compare to the maximum heaving of 5.55% observed in the oedometer the soil in EK-equipped circular and rectangular models showed the heaving of 5.42% and 4.21% respectively. The heaving pressure recorded for the oedometer was 67.5 t.m^{-2} while for the circular and rectangular models these values were 37.7 t.m^{-2} and 18.8 t.m^{-2} respectively. Further, the value of unconfined compressive strength of soil decreases from 141 kPa to 80 kPa after interaction with alkali and the decrease was more prominent in the circular EK model. However, there was an increase in the friction angle and a decrease in cohesion value after alkali interaction. The structural alteration due to alkali solution was examined by SEM and XRD analysis.
.

INTRODUCTION

Electrokinetic (EK) is a newly developed technique for soil stabilization. Casagrande first introduced this method in 1940 to stabilize railway embankments (Casagrande 1949). This technique is based on three basic principles, electromigration, i.e., transport of material due to movement of charged ions, electrophoresis i.e., movement of dispersed particles, and electroosmosis i.e., movement of pore fluid across a porous material. Since the movement of fluid is a big challenge in the case of heterogeneous or low permeable soil, all these phenomena involve the application of voltage gradient across the material. The electrokinetic technique is the best suitable method for injecting pore fluids in such soils under a potential gradient (Alshawabkeh & Bricka 2000).

For in-situ stabilization of soil/sites, the EK technique can be a great option for civil engineers. It may involve minimal disturbance to the existing structures, unlike conventional methods, which are expensive, time-consuming, and maybe challenging to implement at developed sites. The potential of the EK technique is being investigated by several researchers in context to their vital role in various geotechnical solutions such as rapid dewatering of clayey soil which have very high moisture retention capacity (Dizon & Orazem 2020, Jian et al. 2019, Liu et al. 2018, Martin et al. 2019, Shang 1997, Shen et al. 2020) chemical stabilization of low shear strength soil (Estabragh et al. 2019, 2020, Moayedi et al. 2014, Nordin et al. 2013, Lakshmi & Sivaranjani 2014), bio-grouting of soft soil to improve its geotechnical properties (Keykha & Asadi 2017, Keykha et al. 2014, 2015) and removal of heavy metals from the soils (Cameselle et al. 2021, Kim et al. 2001, Ma et al. 2018, Sivapullaiah et al. 2015, Yi et al. 2017). The efficiency of the EK technique is a function of several parameters such as the electrode materials (Méndez et al. 2012, Xiao & Zhou 2019), spacing between the electrode (Rittirong et al. 2008, Turer & Genc 2005, Wan et al. 2021), voltage gradient (Fu et al. 2019, Mu'azu et al. 2016) and rate of chemical addition. It has been reported that out of metals and non-metals which are generally used as electrodes, metal electrodes are more efficient. However, it also has several drawbacks, such as its proneness to corrosion on exposure to an acidic environment which may also lead to soil pollution. To overcome such problems, several experimental investigations were carried out by wrapping the electrodes with polymeric materials. Among various materials, geotextiles were proved to be satisfactorily efficient in reducing the

corrosion of the electrodes (Azhar et al. 2018, Glendinning et al. 2005).

Furthermore, alkali contamination in soils is also a problem that has been receiving great concern owing to its detrimental effects on the existing structures. Alkali contamination causes heaving of the soils and may also impact their engineering properties (Ashfaq et al. 2019, Irfan et al. 2018; Reddy et al. 2017, Vindula & Chavali 2018, Vindula et al. 2019). It has also been reported that alkali contamination causes mineralogical and morphological changes in the soil matrix (Chavali et al. 2017, Sivapullaiah & Manju 2005, Sivapullaiah et al. 2010). A number of works have been reported to study alkali-induced heaving (Chavali et al. 2017, Reddy et al. 2017). All the studies reported till now were conducted at small scale set up in oedometer apparatus. But in practical scenarios, there can be significant variations in the implementation of the process and the results too. For instance, inundation of alkali solution through the soil specimen is possible on a small scale. However, in large-scale models, fluid transport through the sample can be difficult because of the low permeability of the soil. To the author's knowledge, no work has been conducted till now to study the alkali-induced heaving of soil using the EK technique in a large-scale model.

In this paper, an attempt has been made to conduct EK equipped large-scale model study to analyze the heaving phenomena observed in fields. The effect of the model geometry has also been taken into account by using a rectangular and circular-shaped model. The results were compared in terms of percentage heaving and heaving pressure. Further, the effect of boundary geometry in EK-equipped models was analyzed in terms of variations in voltage. The effect of alkali interaction using the EK technique on the engineering properties of the soil was also compared for both models.

MATERIALS AND METHODS

Soil

In the present study, the soil samples were collected by open excavation upto a depth of 3 m from the natural ground level at the Banaras Hindu University Campus. Wet sieving was performed in which the soil sample was first washed through a 75μm sieve and the fraction coarser and finer than 75μm were collected and oven dried separately. Following it, mechanical sieving and hydrometer methods were used as per (Astm D6913-04R2009 2004) to analyze coarser fractions and finer fractions respectively. A semi-log curve was plotted between the percentage finer and diameter of a particle in mm as shown in Fig. 1. Based on the Unified Soil Classification System (USCS), the soil was classified as CL (Clay with low plasticity). Before the experiment, the collected soil samples were oven-dried and sieved. The physical properties
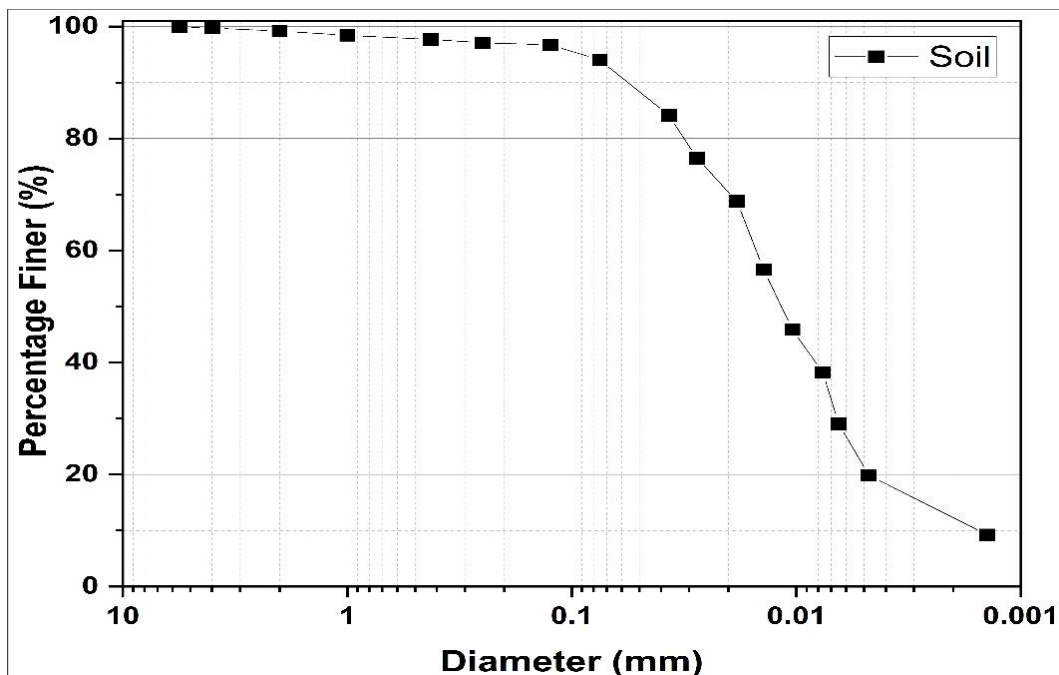
Fig. 1: Particle size distribution curve of soil.

Table 1: Geotechnical properties of test soil.

Property	Soil	Standards
Specific Gravity	2.5	ASTM D854 - 14
Liquid limit (%)	35	ASTM D4318 - 17
Plastic limit (%)	22.23	
Plasticity index (%)	12.77	
Clay	12	ASTM D6913 / D6913M - 17
Silt	80	
Sand	8	
Maximum dry density (g.cc^{-1})	1.66	ASTM D698-12
Optimum moisture content (%)	16.4	
Unconfined compressive strength (kPa)	141.25	ASTM D2166 / D2166M - 16
Cohesion (kPa)	55	ASTM D2850 - 15
The angle of friction (º)	13	

Table 2: Chemical composition of test soil (XRF analysis).

Mineral	SiO_2	Al_2O_3	TiO_2	Fe_2O_3	MnO	MgO	CaO	Na_2O	K_2O	P_2O_5
Percentage Composition	62.6	15.89	0.81	7.55	0.06	7.36	0.65	0.36	3.53	0.07

and chemical composition of soil are listed in Table 1 and Table 2 respectively.

Experimental Set-up and Test Procedure

The whole experimental analysis was conducted in three different sets up the details of each type of experimental setup are explained in detail in the subsequent sections.

Oedometer Test

One dimensional free swell test was performed in Oedometer in accordance with ASTM D2166 (2020) to study the heaving behavior of soil inundated with 16 M NaOH solution. The virgin soil was compacted in the consolidation ring of 6 cm diameter and 2 cm height at the density corresponding to the optimum moisture content. Porous stones with filter papers were placed on both sides of the soil specimen extruded in the ring after compaction, which is then placed into the oedometer assembly. The soil sample is inundated with 16
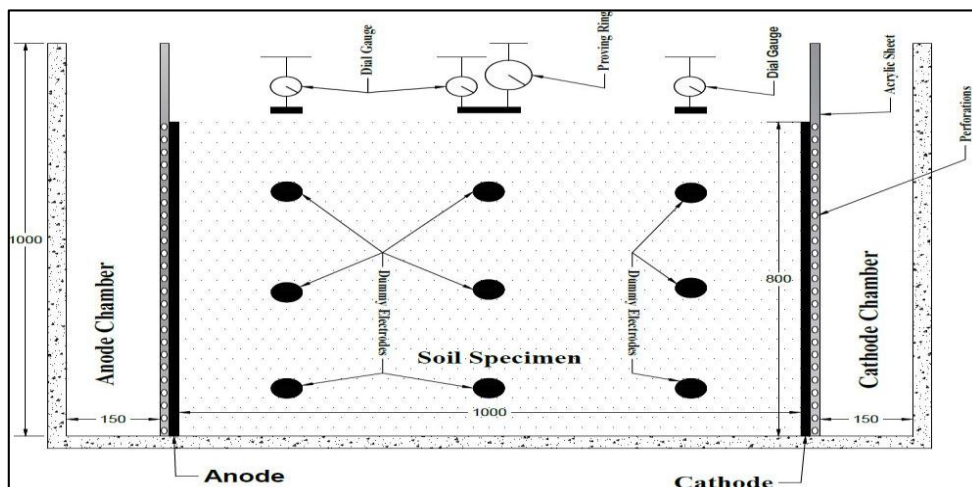
Fig. 2: Elevation view of the rectangular electrokinetic model.

M NaOH solution and is kept free from any type of load application. Here, in this case, the flow of NaOH as the pore fluid takes place without the effect of any potential gradient. Soon after the interaction with NaOH, the soil starts heaving. The amount of heaving in the vertical direction with the time was recorded using a dial gauge. The test was continued till the time no significant change in dial gauge reading was observed with time. The percentage heaving in the vertical direction was then calculated as the ratio of the actual heaving to the initial height of the specimen.

The principle mechanism behind heaving due to alkali interaction is the increase in the pH of the soil which leads to an increase in negative charge on the surface of the soil. These charges create greater repulsion between the soil particles and thus cause heaving (Paulose et al. 2017).

Rectangular Electrokinetic Model

The second phase of the experiment involved a large-scale model testing in studying the heaving behavior of alkali-interacted soil. The movement of the NaOH as the pore fluid takes place under the influence of an electric potential gradient. The schematic of the elevation and plan of the model testing tank has been shown in Fig. 2 and Fig. 3. Fig. 4 shows the image of a rectangular EK model showing the position of the dummy electrode, dial gauge, and proving ring. The testing tank was rectangular with dimensions of 1300 mm × 750 mm × 1000 mm fabricated brick masonry. The tank was divided transversally into three parts comprising three chambers, namely, the anode chamber, the cathode chamber, and the soil chamber. The length of the soil chamber was 1000 mm,

while that of both the electrolyte chambers was 150 mm. A 20 mm thick perforated acrylic sheet was placed between the electrolyte chamber and soil chamber to ensure a uniform flow of the electrolyte. The top surface was kept open where the soil heaving was measured. The electrodes were made up of a brass net sandwiched between two geotextile sheets which were then fixed against the acrylic sheets. This brass net was used to apply a voltage gradient between the anode and cathode. A potential difference of 100 V across the two ends of the soil chamber was maintained throughout the experiment. The effect of NaOH on the percentage heaving, heaving pressure, voltage, unconfined compressive strength, and shear behavior of the soil was evaluated across the soil specimen.

Dial gauges were placed at nine different locations at the top soil surface as shown in Fig. 4(b), to measure the surface heaving. The nine-dial gauge was placed in sets of three at a distance of 250 mm, 500 mm, and 750 mm from the anode. Three proving rings were placed at the central line to measure the heaving pressure exerted by the soil. The voltage sensors 9 in number, were placed inside the soil sample to measure voltage and temperature change throughout the experiment as shown in Fig 4(a). The voltage sensors can be regarded as dummy electrodes.

Circular Electrokinetic Model

The third phase of the experiment was conducted in a large-scale circular model made of RCC, the elevation and plan of which are shown in Fig. 5 and Fig. 6, respectively.

The anode, cathode, and soil chambers were in the form of three concentric compartments. The outermost chamber
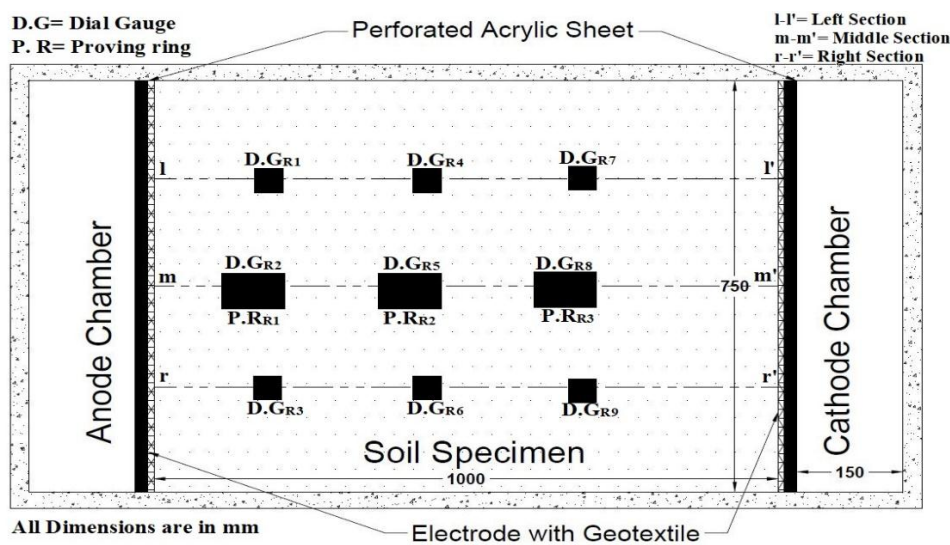
Fig. 3: Plan view of the rectangular electrokinetic model.

Fig. 4: Rectangular EK model image (a) Soil chamber installed with dummy electrode (b) Soil chamber with D.G. and P.R.

was the anode chamber. The middle compartment was for soil specimens, while the inner compartment was the cathode chamber. The diameter of the soil compartment and anode chamber was 600 mm and 150 mm, respectively, as shown in Fig. 6, while the height of the tank was 750 mm. The flow of the fluid was radially inwards from the anode chamber to the cathode chamber. Perforations were made on the walls of the anode chamber for the uniform flow of solution. Like

in the case of a rectangular setup, the electrodes were made by sandwiching a brass net between two Geosynthetic sheets and were placed on the inner wall surface of the soil chamber.

Fig. 7 shows the image of a circular EK model with a dummy electrode, dial gauge, and proving ring. Dial gauge and proving rings were placed at the top surface of the soil for measuring the heaving and heaving pressure, respectively. As
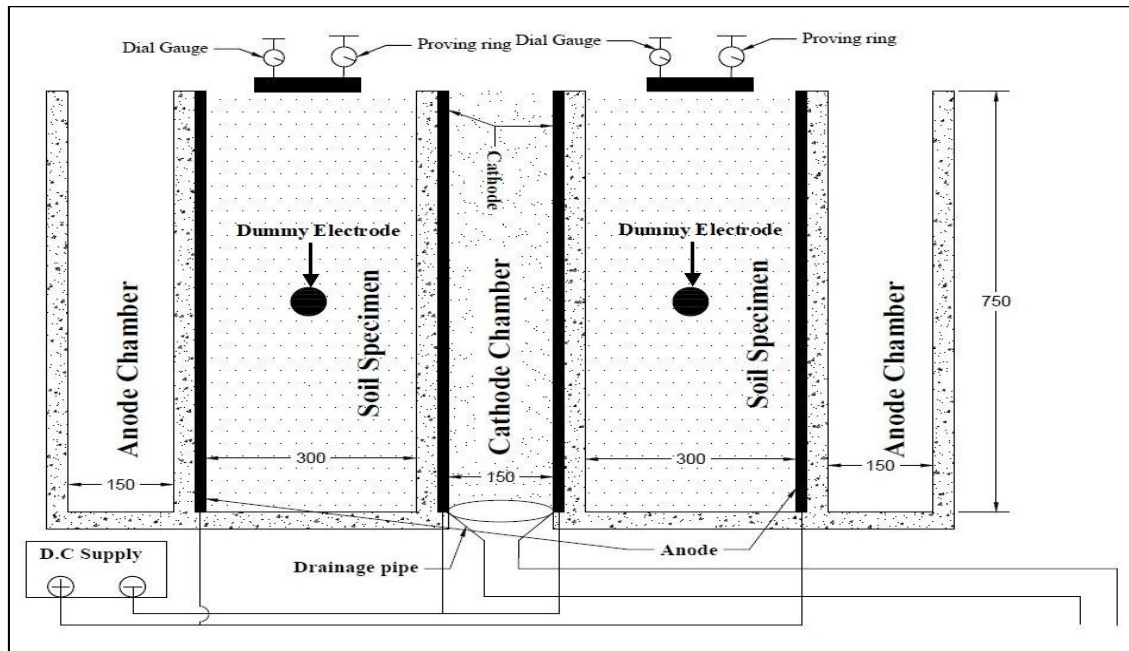
Fig. 5: Elevation view of a circular electrokinetic model.

can be seen from Fig. 7(c), the four dial gauges were placed at the mid-point of the anode and cathode. Furthermore, four voltage sensors were placed at the mid-depth just below the four dial gauges to monitor the change in the voltage and temperature sensors as shown in Fig 7(b). The cathode chamber was connected to a drain pipe at the bottom from where the electrolyte was drained out at regular intervals, while the anode chamber was refilled at regular intervals.

Sample Preparation

Preparation of the soil bed in the testing tank was a challenging task as any sort of non-homogeneity was not desirable. The soil bed was prepared at the bulk density corresponding to the optimum moisture content. A pre-calculated amount of soil was mixed with the water corresponding to the OMC, and this soil was compacted in the tank in 5 layers. The bottom two layers were given a little less compactive effort as compared to the upper one to incorporate the settlement due to overburden stresses. Once the soil bed was prepared, Cone Penetration Test (CPT) was conducted at different locations to check for uniformity in the prepared soil bed. The results were plotted in terms of penetration of the cone in mm per blow which is termed as Dynamic Penetration Index (DPI). In the case of the rectangular tank, CPT tests were conducted at the four corners, while in the case of the circular tank, it was conducted at two diametrically opposite
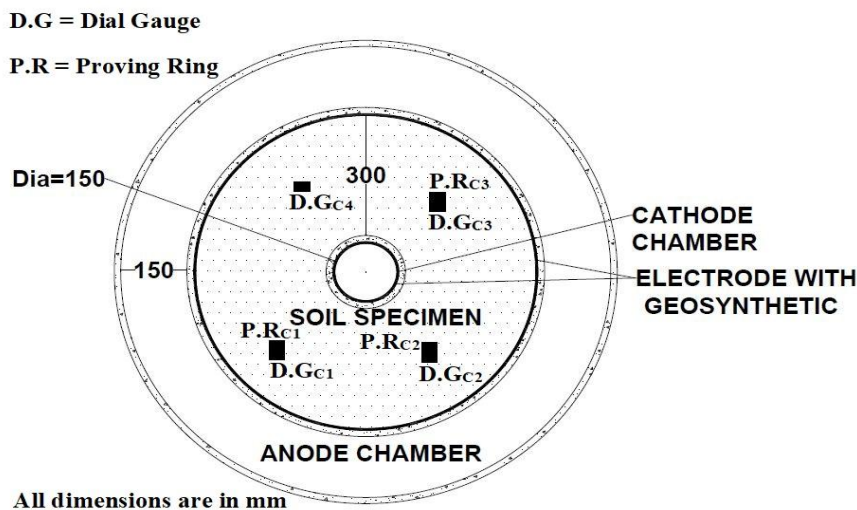
Fig. 6: Plan view of circular EK model.
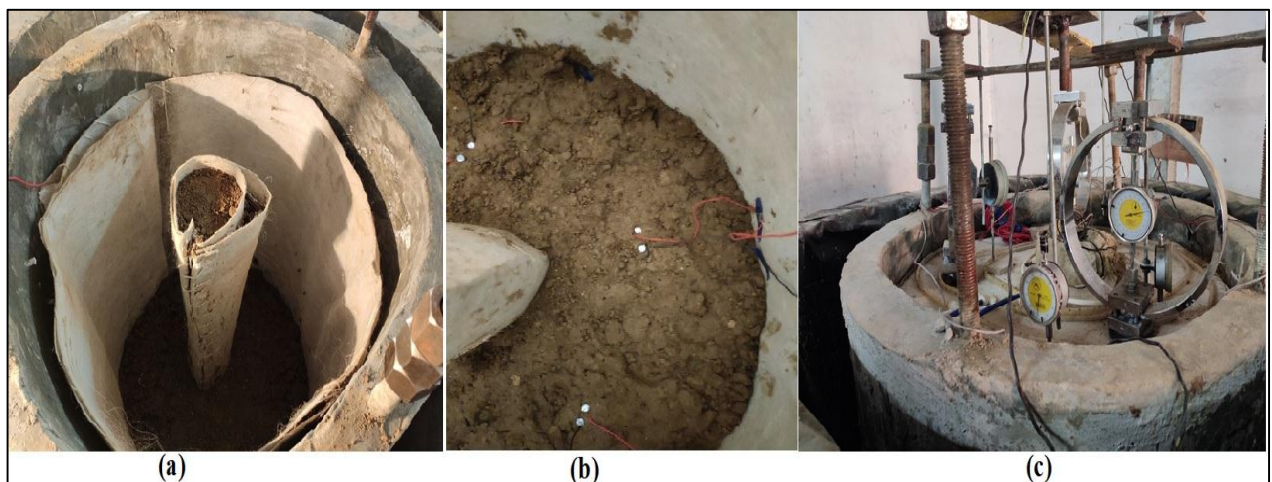
Fig. 7: Circular EK model (a) soil chamber (b) soil with dummy electrode (c) soil with D.G and P.R.

points. The results of the tests are shown in Fig. 8. Fig. 8(a) shows the CPT results for the rectangular model, while Fig. 8(b) shows the CPT results for the circular model. The CPT profiles for both types of the model were almost uniform for all locations except a slight decrease was observed at the bottom owing to the densification due to overburden stresses.

RESULTS AND DISCUSSION

Surface Heaving

The time vs heaving profiles for all the three test setups are shown in Fig. 9, Fig. 10, and Fig. 11. The soil sample was mixed thoroughly with distilled water at optimum moisture content and compacted statically to the desired depth to achieve density nearest to maximum dry density. Fig. 9 shows the percentage heaving with time recorded in the oedometer tests. The heaving showed a continuous increase with time.
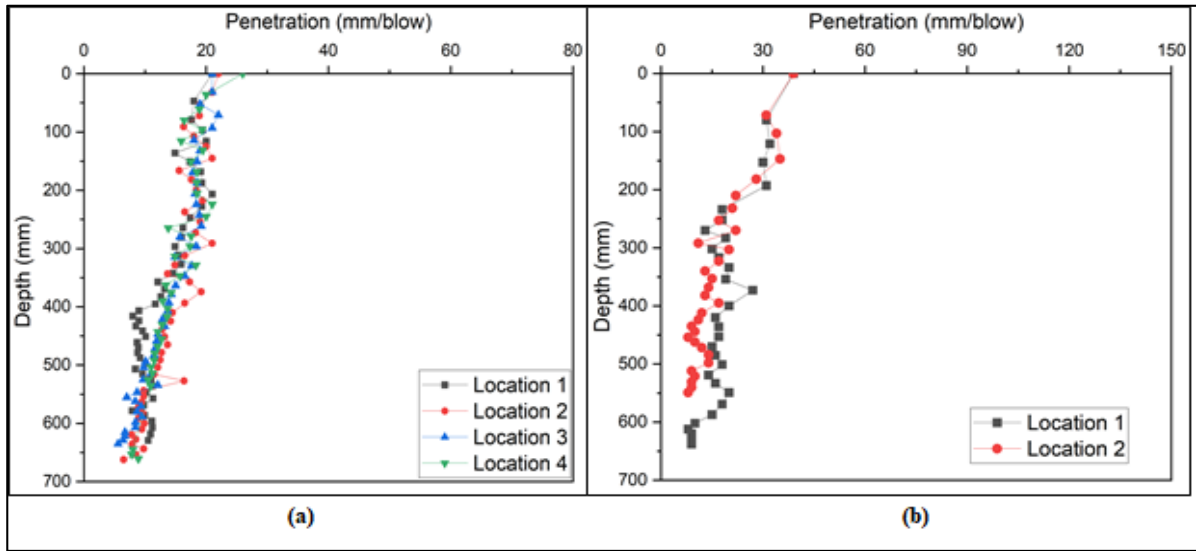
Fig. 8: CPT Test results for (a) Rectangular model and (b) Circular model.
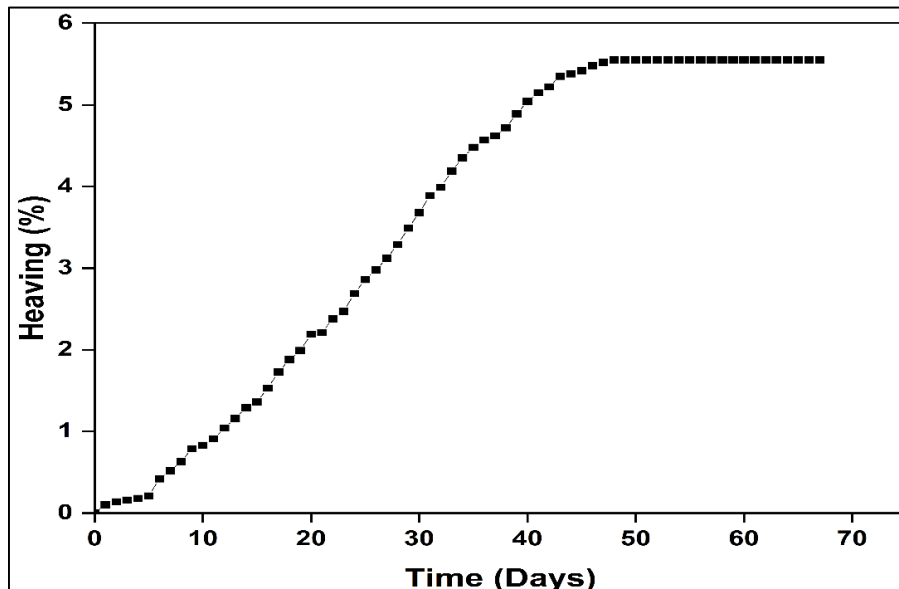
Fig. 9: Heave in soil inundated with 16 M NaOH solution in Oedometer test.

The maximum percentage of heaving was 5.55% which was achieved in approximately 40 days after which no significant heaving was observed. Similarly, Fig. 10 shows the heaving recorded in the nine-dial gauges in the rectangular electro-kinetic test setup. The graph is evidence of an obvious increase in the heaving with time for all the dial gauges. However, when the distance from the anode was increased, the percentage of heaving decreased. The maximum value of heaving in the case of rectangular test setup was 4.39% which was observed in the dial gauges nearest to the anode. The reason could be attributed to the fact that the soil nearer to the anode gets rapidly interacted with NaOH as the flow of the electrolyte is from anode to cathode. Further, it was

also observed that the heaving shown by the dial gauges at the edges was slightly higher than those at the middle for a fixed distance from the anode. The possible reason behind this particular observation could be that the flow of electrolytes along the model boundaries would be faster due to less resistance offered at the soil-boundary interface. The time-heaving profile obtained from the four dial gauges in the circular test setup is shown in Fig. 11. It was seen that the heaving in the case of the circular electro-kinetic model was increasing sharply with increasing interaction time. The maximum heaving observed, in this case, was 5.42%. The heaving in the four dial gauges did not show much deviation since the radial inward flow of electrolyte causes uniform
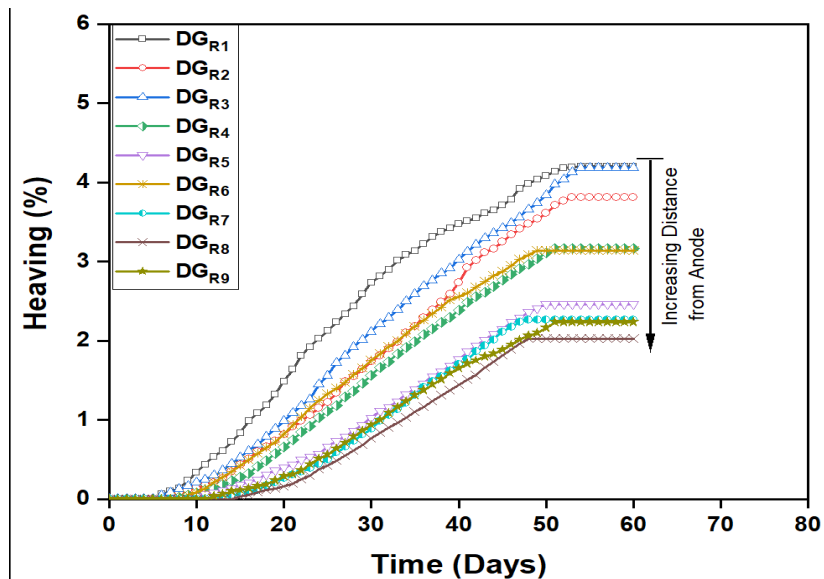
Fig. 10: Heave in soil inundated with16 M NaOH solution in rectangular EK model.
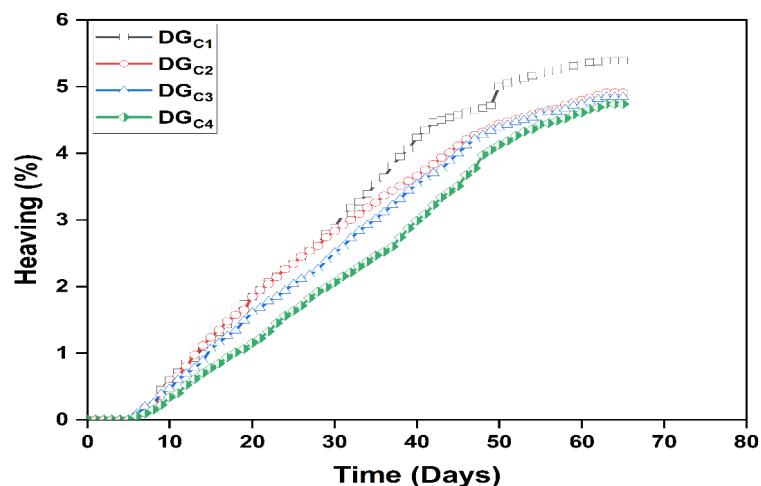
Fig. 11: Heave in soil inundated with16 M NaOH solution in circular EK model.

soil-alkali interaction at a particular radial distance from the anode.

It is also worth noticing that the rate of heaving, represented by the slope of the time-heaving curves, is maximum in the case of the circular model where the electrolyte flow was radial. Moreover, the rate of heaving in the case of an oedometer increases initially and becomes constant after 25-30 days. In the case of the rectangular model, the rate of heaving increases initially up to 30-35 days, reduces thereafter, and becomes constant after 50-55 days. Unlike in the above two experiments, the rate of heaving in the case of the circular model shows a sharp increase with time and did not show any reduction up to 60 days.

A comparison of the percentage heaving in the case of all the three setups is shown in Fig. 12. From the fig. it can be observed that the percentage heaving was maximum in the case of the oedometer test followed by the circular EK model and then the rectangular EK model. When heave is considered, the soil weight contributes an additional component of vertical load (Merifield et al. 2009). It could be possible that in the case of the large-scale EK models, a portion of the heaving at the bottom layers is suppressed by the overburden pressure of the overlying soil. This effect would not be prominent in the case of an oedometer as a relatively very less amount of soil is used in the specimen.

Heaving Pressure

The heaving pressure in EK models was measured through a proving ring which is placed on the surface at three different locations which are already shown in their respective plans. On the other hand, the heaving pressure in the oedometer is the total amount of load required to bring back the deflection in the dial gauge to its original position. A comparative bar chart depicting the heaving pressure obtained for all both EK tests is shown in Fig.13. Again, the maximum heaving pressure was observed in the oedometer test which is 67.5 $t.m^{-2}$ while the heaving pressure in the circular EK model and rectangular EK model is about 37.8 $t.m^{-2}$ and 18.8 $t.m^{-2}$ respectively. The heaving pressure in all three proving rings in the circular model is approximately the same while in the case of the rectangular model, the heaving pressure reduces as the distance from the anode increases.

Comparison of Rectangular and Circular EK Model

The sections that follow give a comparison of the variation of the various factors in the rectangular EK model and the circular EK model.

Variation of Electric Potential

The plot of the electric potential versus time as measured during the EK tests in rectangular and circular EK models are shown in Fig. 14 and Fig. 15 respectively. The electric potential was measured using voltage sensors at the mid-depth just below the dial gauges. Fig.14 shows the variation of electrical potential in the rectangular EK model. The recorded electric potential showed a decrease in moving from anode to cathode. The electric potential increases as the flow start from the anode to the cathode and then decreases with the precipitation of sodium ions across the soil specimen.
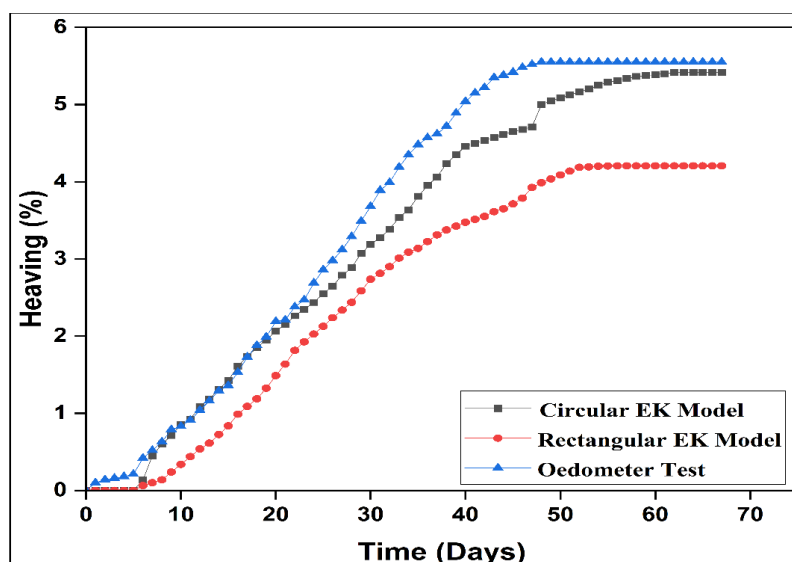
Fig. 12: Effect of model boundaries on percentage heaving.
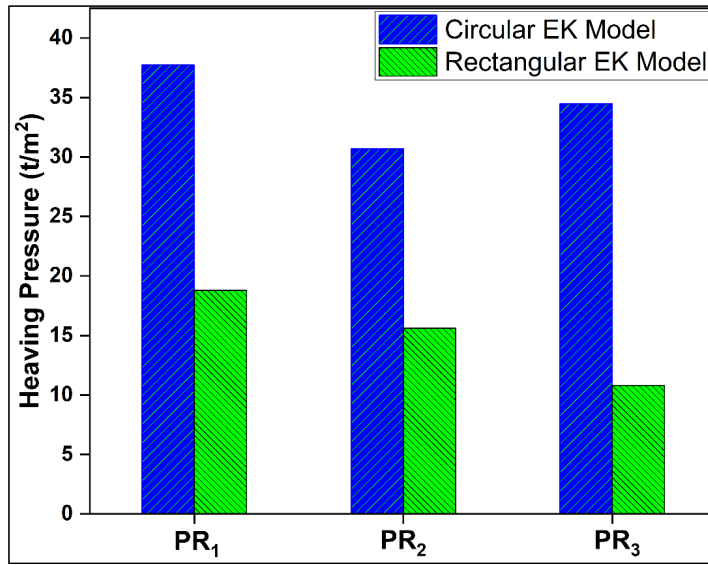
Fig. 13: Heaving pressure in soil due to alkali interaction in EK tests.
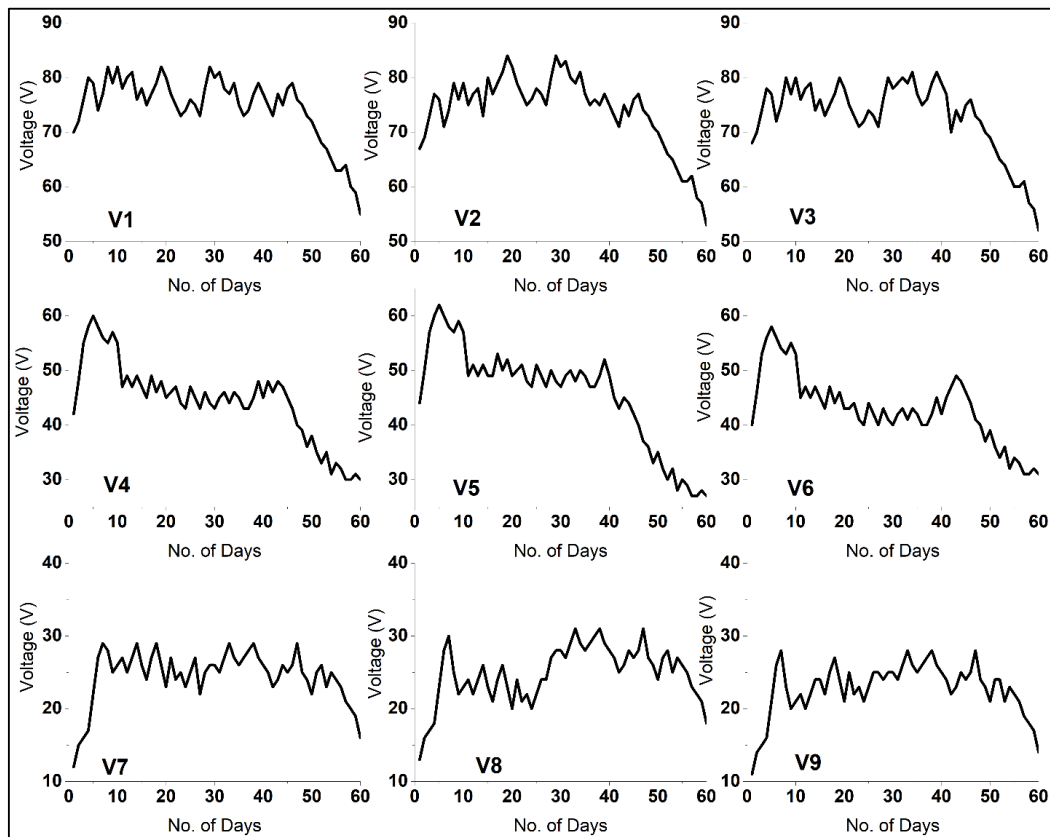
Fig. 14: Variation of Electrical potential in rectangular EK model.

However, a non-uniformity in electric potential variation was observed due to the non-uniform flow of electrolytic solution in the soil sample. This non-uniformity in flow may occur due to the large volume of soil and non-uniform precipitation of sodium ions in the soil sample.

Likewise, Fig. 15 depicts that in the circular EK model, a similar electric potential profile was observed with time for all four locations which indicates the uniformity in flow at every location. As the experiment continues, the electrical potential increases due to the movement of ions from the anode to the cathode. After 15 days, a linear decrement in electrical potential was observed with time which occurs due to the precipitation of sodium hydroxide into the soil. After the precipitation of sodium hydroxide, the electric potential becomes constant across the soil sample. Therefore, it is apparent that the change in electrical potential of the circular EK model was approximately the same, however in the rectangular EK model the electrical potential varies as we move from anode to cathode.

Unconfined Compressive Strength

The unconfined compressive strength (UCS) test was conducted in accordance with ASTM D2166 (2016) to analyze the change in the strength of soil specimens after alkali interaction. The UCS value of the virgin soil conducted before its interaction with NaOH was found to be 141 kPa. Fig. 16(a) shows the UCS values of alkali interacted soil in a circular EK model collected from the mid-depth below the location of dial gauges. The UCS value was in the range of 84-93 kPa for all four specimens after an interaction period of 60 days. Similarly, Fig. 16(b) shows the UCS value of alkali interacted soil in a rectangular EK model collected from the mid-depth below the location of dial gauges. The UCS values were in the range of 90 to 124 kPa after an interaction period of 60 days. The samples collected from the mid-section showed the highest UCS value as compared to the left and right sections. This particular observation can be related to the percentage of heaving where the lowest heaving was observed at the midsection.

The reduction in UCS value with respect to virgin soil after alkali interaction can be attributed to the dissolution of clay minerals in an alkaline environment and the formation of new compounds (Sivapullaiah & Manju 2005). From the UCS graph of circular and rectangular EK models, it was
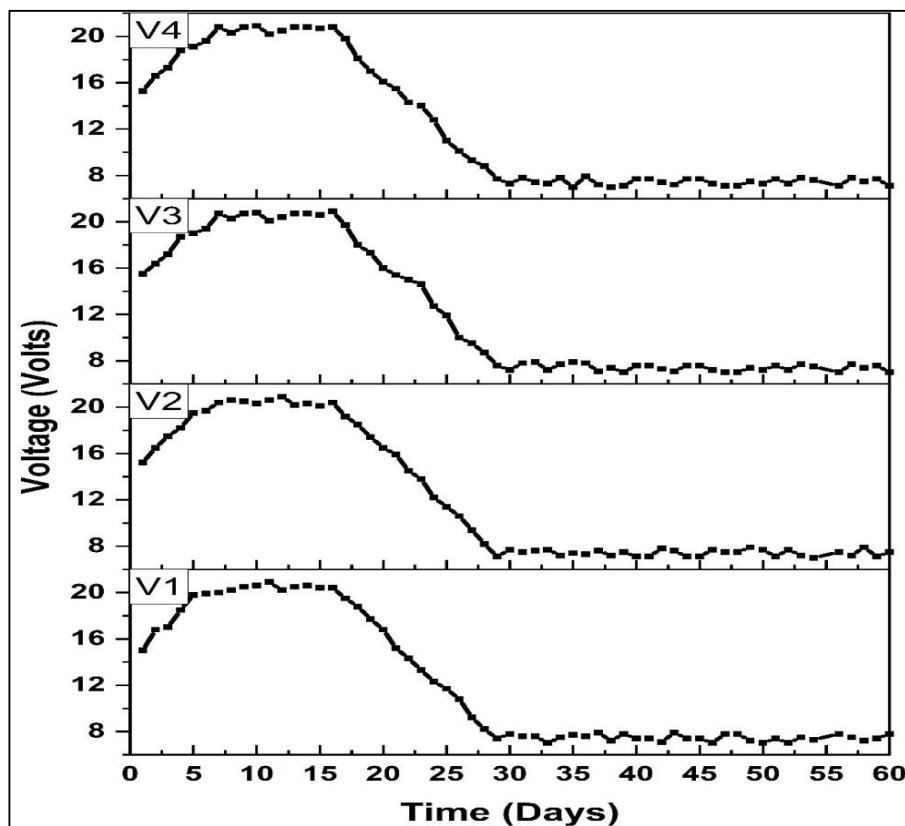
Fig. 15: Variation of Electrical potential in circular EK model.

also observed that the UCS value in the circular model at all four sampling points was similar whereas, in a rectangular model, the reduction in the UCS values was less pronounced on moving from anode to cathode. This was because the intensity of the alkali interaction was not the same at all the points at a given time as the flow of electrolyte from anode to cathode causes the electrolyte to reach different sampling points at different times.

Shear Strength Parameters

Unconsolidated Undrained triaxial tests were also conducted in accordance with ASTM D2850 (2015) at the collected specimens at three confining stresses of 50 kPa, 100 kPa, and 150 kPa. The shear strength parameters calculated from the obtained results for the rectangular EK model are shown in Fig. 17. Fig.17 (a) shows the variation of friction angle with the distance from the anode along all three sections. The cohesion and internal friction angle of an un-interacted soil sample is obtained at 55 kPa and 13º. The interaction of NaOH causes an increase in the friction angle. The friction angle is reduced as the distance from the anode increases. Furthermore, the cohesion decreased as the interaction of the NaOH increased as can be seen from Fig. 17(b). Higher decrement in cohesion values was found for the samples nearer to the anode. These
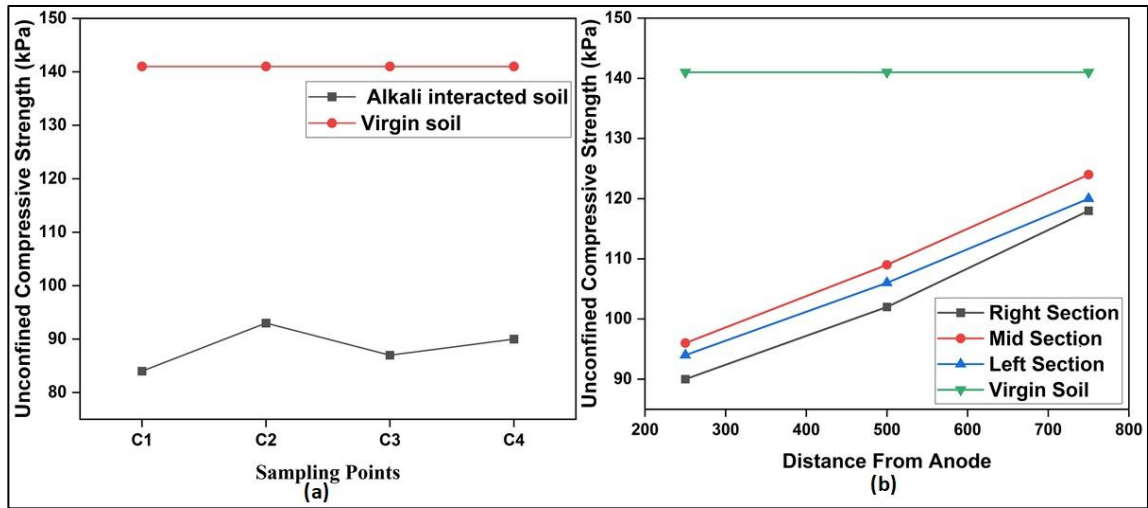
Fig. 16: Variation of UCS in (a) circular EK model and (b) rectangular EK model.
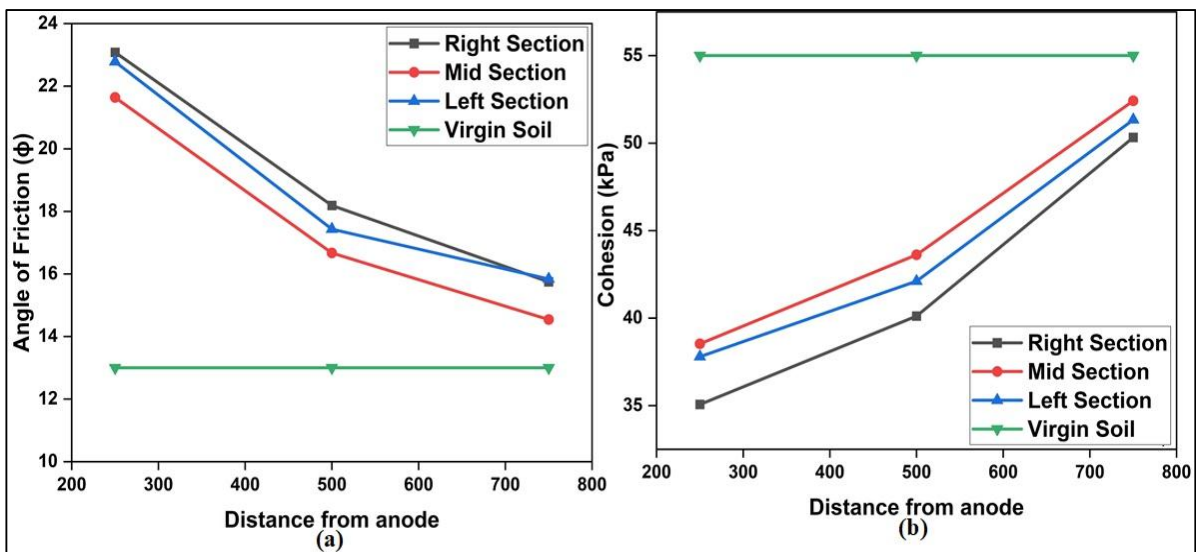
Fig. 17: Variation of (a) Angle of Friction (b) Cohesion in rectangular EK model.

changes in cohesion values decrease as the distance from the anode increases. Similarly, Fig. 18(a) and Fig. 18(b) show the variation of friction angle and cohesion respectively for the circular EK model. The values of friction angle and cohesion were almost similar for all the soil samples. However, there was a definite change in the cohesion as well as in the friction angle of the soil after its interaction with NaOH.

In an attempt to find the possible reason behind such a change in the friction angle and cohesion, it was realized that the pH value is a vital parameter that may potentially influence the mechanical response of the clayey soils. As reported by (Gratchev & Sassa 2009), the edge surface of the clay particle is highly dependent on pH. In a highly alkaline medium when pH is very high, these edges become more negative due to the adsorption of OH^- ions. This induces the face-to-face association of the particles which is responsible for the change in the shear strength parameters.

Scanning Electron Microscopy

The morphological changes in the soil matrix under alkali interaction were studied by scanning electron microscopy. After the interaction period of 60 days, samples were collected for SEM analysis. The SEM images of the virgin soil and the soil interacting with 16M NaOH solution are shown in Fig. 19. Distinct flaky particle structure of the virgin soil can be observed in Fig 19 (a). The SEM image of soil interacting
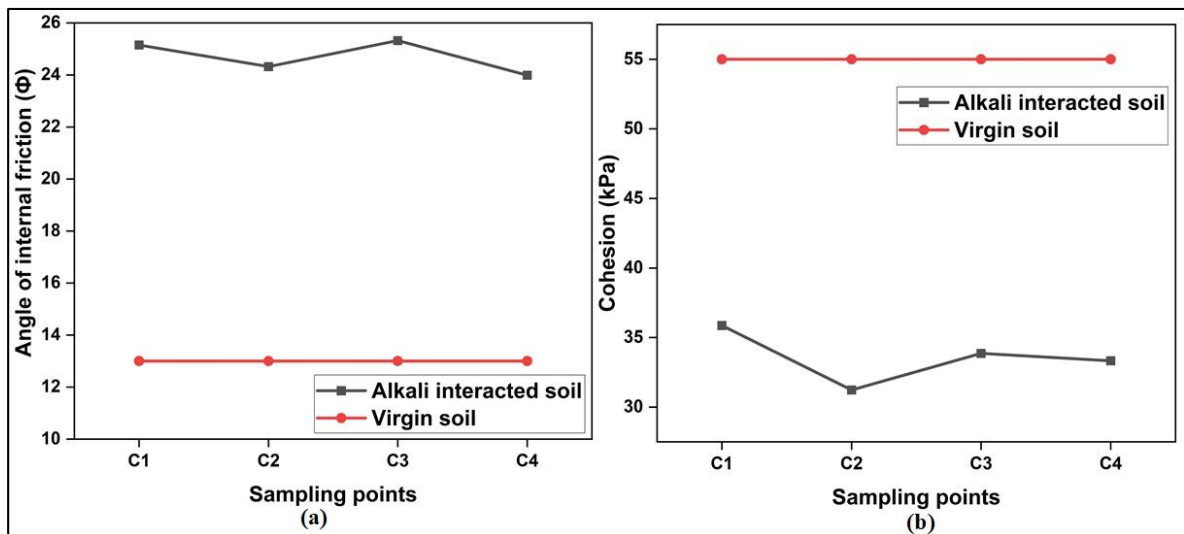
Fig. 18: Variation of (a) Angle of Friction (b) Cohesion in circular EK model.
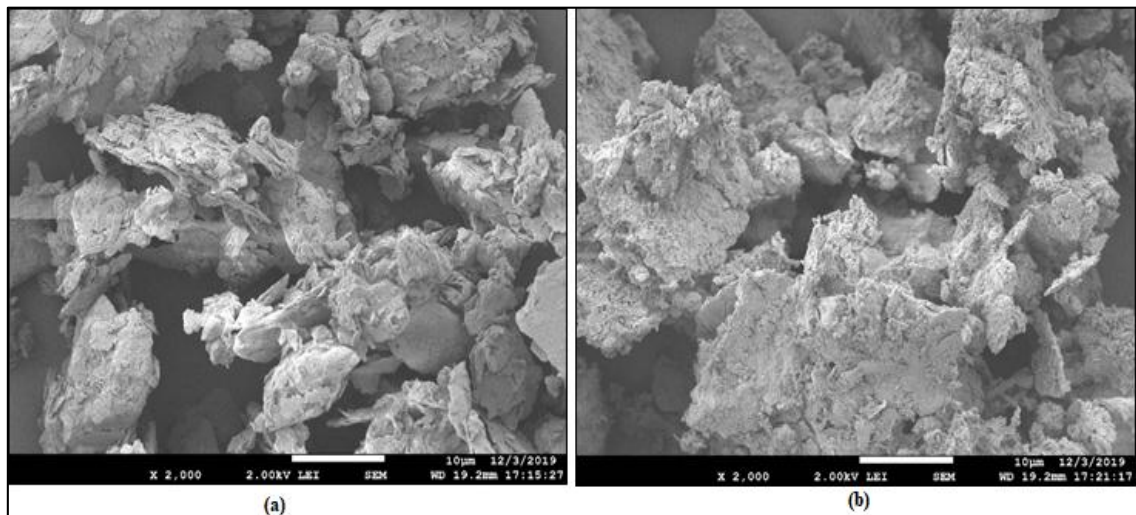
Fig. 19: SEM images of virgin soil (a) Virgin soil (b) Alkali interacted soil.

with alkali shown in Fig. 19(b) shows some disintegration or weathering. This morphological change in the soil supports the formation of a new compound due to alkali interaction which causes heaving.

X-ray Diffraction Analysis

XRD analysis was performed to check for the formation of any new products in the soil after its interaction with the 16M NaOH solution. The soil specimens were collected soon after the completion of the 60 days interaction period. These specimens were dried and ground to a fine powder with a mortar and pestle. X-ray diffractometer was used to scan the sample and identify the mineral composition of the soil specimen corresponding to XRD peak position and intensities using JCPDS software. The X-Ray diffraction patterns for virgin and alkali interacted soil are shown in Fig 20. New peaks corresponding to NASH have been observed by the XRD analysis which is a mineral of zeolite group (Sodium aluminum silicate hydrate) which is responsible for the heaving of soil.
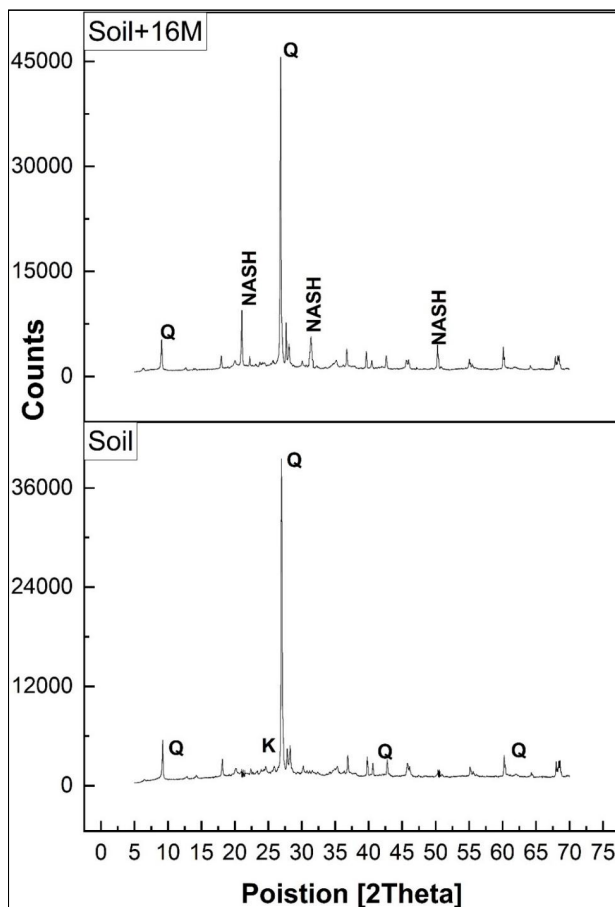
Fig. 20: X-ray diffraction analysis of soil and soil inundated with 16 M NaOH solution.

CONCLUSIONS

The following conclusions can be drawn from the experimental analysis conducted in the present study:

- Interaction of soil with an alkali causes an unexpected heaving in the soil in the soil. The maximum percentage of heaving due to alkali interaction was observed in the oedometer test followed by the circular EK model and rectangular EK model. More uniform alkali interaction was achieved in the case of the circular EK model when compared to the rectangular EK model in low permeable soil.

- A considerable decrease in the unconfined compressive strength of the virgin soil was observed after its interaction with the alkali solution. In the case of the rectangular EK model, the effect of alkali on the UCS value was reduced as the distance from the anode was increased.

- Variation of electrical potential with time in the soil shows the flow of alkali solution into the soil is uniform in the case of the circular EK model.

- Alkali interaction causes an increase in the friction angle and a decrease in cohesion value. The respective change was directly proportional to the intensity of the alkali interaction which is a function of the time of interaction and flow of the electrolyte.

REFERENCES

Alshawabkeh, A.N. and Bricka, R.M. 2000. Basics and applications of electrokinetic remediation. Environ. Sci. Pollut. Control Ser., 61: 95-112.

Ashfaq, M., Heeralal, M. and Reddy, P.H.P. 2019. A Study on Strength Behavior of Alkali-Contaminated Soils Treated with Fly Ash: Recycled Waste Materials. Springer, Singapore., pp. 137-143.

ASTM D2166/D2166M. 2016. Standard Test Method for Unconfined Compressive Strength of Cohesive Soil. The Annual Book of ASTM Standards, PA., 1-6.

ASTM D2166/D2166M. 2020. Standard Test Methods for One-Dimensional Consolidation Properties of Soils. The Annual Book of ASTM Standards, PA., 1-10.

ASTM D2850. 2015. Standard test method for unconsolidated-undrained triaxial compression test on cohesive soils. ASTM International, West Conshohocken, PA, USA.

ASTM D4318. 2010. Standard Test Methods for Liquid Limit, Plastic Limit, and Plasticity Index of Soils. ASTM International, West Conshohocken, PA. 1-14.

ASTM D6913-04R. 2009. Standard Test Methods for Particle-Size Distribution (Gradation) of Soils Using Sieve Analysis. ASTM International, West Conshohocken, PA., 61-35.

ASTM D698. 2003. Standard Test Methods for Laboratory Compaction Characteristics of Soil Using Standard Effort. The Annual Book of ASTM Standards, PA., 1-11.

ASTM D854. 2000. Standard Test Methods for Specific Gravity of Soil Solids by Water Pycnometer. ASTM International, West Conshohocken, PA. 1-7.

Azhar, A.T.S., Jefferson, I., Madan, A., Abidin, M.H.Z. and Rogers, C.D.F.

2018. Electrokinetic stabilization method of soft clay in the pure system using the electrokinetic geosynthetic electrode. J. Phys. Conf. Ser., 995(1): 012109.

Cameselle, C., Gouveia, S. and Cabo, A. 2021. Enhanced electrokinetic remediation for the removal of heavy metals from contaminated soils. Appl. Sci., 11(4): 1799.

Casagrande, I.L. 1949. Electro-osmosis in soils. Geotechnique, 1(3): 159-177.

Chavali, R.V.P., Vindula, S.K., Babu, A. and Pillai, R.J. 2017. Swelling behavior of kaolinitic clays contaminated with alkali solutions: a micro-level study. Appl. Clay Sci., 135: 575-582.

Dizon, A. and Orazem, M.E. 2020. Advances and challenges of electrokinetic dewatering of clays and soils. Curr, Opinion Electrochem., 22: 17-24.

Estabragh, A.R., Moghadas, M., Javadi, A.A. and Abdollahi, J. 2019. Stabilization of clay soil with polymers through electrokinetic technique. Euro. J. Environ. Civil Eng., 12: 1-19.

Estabragh, A.R., Moghadas, M., Javadi, A.A. and Abdollahi, J. 2020. Stabilization of clay soil by ion injection using an electrical field. Proceed. Instit. Civil Eng. Ground Improve., 15: 1-13.

Fu, H., Yuan, L., Wang, J., Cai, Y., Hu, X, and Geng, X. 2019. Influence of high voltage gradients on electrokinetic dewatering for Wenzhou clay slurry improvement. Soil Mech. Found. Eng., 55(6): 400-407.

Glendinning, S., Jones, C.J. and Pugh, R.C. 2005. Reinforced soil using cohesive fill and electrokinetic geosynthetics. Int. J. Geomech., 5(2): 138-146.

Gratchev, I.B. and Sassa, K. 2009. Cyclic behavior of fine-grained soils at different pH values. J. Geotech. Geoenviron. Eng., 135(2): 271-279.

Irfan, M., Chen, Y., Ali, M., Abrar, M., Qadri, A. and Bhutta, O. 2018. Geotechnical properties of effluent-contaminated cohesive soils and their stabilization using industrial by-products. Processes, 6(10): 203.

Jian, Z., Yanli, T., Cunyi, L. and Xiaonan, G. 2019. Experimental study of electro-kinetic dewatering of silt based on the electro-osmotic coefficient. Environ. Eng. Science., 36(6): 739-748.

Keykha, H.A. and Asadi, A. 2017. Solar-powered electro-bio-stabilization of soil with ammonium pollution prevention system. Adv. Civil Eng. Mater., 6(1): 360-371.

Keykha, H.A., Huat, B.B. and Asadi, A. 2014. Electrokinetic stabilization of soft soil using carbonate-producing bacteria. Geotech. Geol. Eng., 32(4): 739-747.

Keykha, H.A., Huat, B.B. and Asadi, A. 2015. Electro-bio grouting stabilization of soft soil. Environ. Geotech., 2(5): 292-300.

Kim, S. O., Moon, S. H. and Kim, K. W. 2001. Removal of heavy metals from soils using enhanced electrokinetic soil processing. Water Air Soil Pollut., 125(1): 259-272.

Lakshmi, P.R. and Sivaranjani, N. 2014. Chemical stabilization of soft clay soil using the electrokinetic method. IOSR J. Mech. Civil Eng., 11(2): 34-37.

Liu, Y., Xie, X., Zheng, L. and Li, J. 2018. Electroosmotic Stabilization on Soft Soil: Experimental Studies and Analytical Models (A historical review). Int. J. Electrochem. Sci., 13: 9051-9068.

Ma, Y., Li, X., Mao, H., Wang, B. and Wang, P. 2018. Remediation of hydrocarbon–heavy metal co-contaminated soil by electrokinetics combined with biostimulation. Chem. Eng. J., 353: 410-418.

Martin, L., Alizadeh, V. and Meegoda, J. 2019. Electro-osmosis treatment techniques and their effect on dewatering of soils, sediments, and sludge: A review. Soils Found., 59(2): 407-418.

Méndez, E., Pérez, M., Romero, O., Beltrán, E.D., Castro, S., Corona, J.L. and Bustos, E. 2012. Effects of electrode material on the efficiency of

hydrocarbon removal by an electrokinetic remediation process. Electrochim. Acta, 86: 148-156.

Merifield, R.S., White, D.J. and Randolph, M.F. 2009. Effect of surface heave on the response of partially embedded pipelines on clay. J. Geotech. Geoenviron. Eng., 135(6): 819-829.

Moayedi, H., Kassim, K.A., Kazemian, S., Raftari, M. and Mokhberi, M. 2014. Improvement of peat using Portland cement and electrokinetic injection technique. Arab. J. Sci. Eng., 39(10): 6851-6862.

Moayedi, H., Kassim, K.A., Kazemian, S., Raftari, M. and Mokhberi, M. 2014. Improvement of peat using Portland cement and electrokinetic injection technique. Arab. J. Sci. Eng., 39(10): 6851-6862.

Nordin, N.S., Tajudin, S.A. and Kadir, A.A. 2013. Stabilization of soft soil using electrokinetic stabilization method. Int. J. Zero Waste Gen., 1(1): 5-12.

Ou, C.Y., Chien, S.C. and Chang, H.H. 2009. Soil improvement using electroosmosis with the injection of chemical solutions: field tests. Canad. Geotech. J. 46(6): 727-733.

Paulose, S., Reddy, P.H.P. and Jayakumar, K.V. 2014. Swell potential studies on soils contaminated with NaOH solutions. Proceed. Indian Geotech. Conf., 18-20.

Reddy, H.P., Prasad, C.R.V. and Pillai, R.J. 2017. Swelling of natural soil subjected to acidic and alkaline contamination. Period. Polytech. Civil Eng., 61(3): 611-620.

Rittirong, A., Shang, J.Q., Mohamedelhassan, E., Ismail, M.A. and Randolph, M.F. 2008. Effects of electrode configuration on electrokinetic stabilization for caisson anchors in calcareous sand. J. Geotech. Geoenviron. Eng., 134(3): 352-365.

Shang, J.Q. 1997. Electrokinetic dewatering of clay slurries as engineered soil covers. Canad. Geotech. J., 34(1): 78-86.

Shen, Y., Shi, W., Li, S., Yang, L., Feng, J. and Gao, M. 2020. Study on the Electro-Osmosis Characteristics of Soft Clay from Taizhou with Various Saline Solutions. Advances in Civil Engineering.

Sivapullaiah, P.V. and Manju, K. 2005. Kaolinite–alkali interaction and effects on basic properties. Geotech. Geol. Eng., 23(5): 601-614.

Sivapullaiah, P.V., Prakash, B.S.N. and Suma, B. N. 2015. Electrokinetic removal of heavy metals from soil. J. Electrochem. Sci. Eng., 5(1): 47-65.

Sivapullaiah, P.V., Sankara, G. and Allam, M.M. 2010. Mineralogical changes and geotechnical properties of an expansive soil interacted with a caustic solution. Environ. Earth Sci., 60(6): 1189-1199.

Turer, D. and Genç, A. 2005. Assessing the effect of electrode configuration on the efficiency of electrokinetic remediation by sequential extraction analysis. J. Hazard. Mater., 119(1-3): 167-174.

Vindula, S.K. and Chavali, R.V.P. 2018. Role of fly ash in control of alkali induced swelling in kaolinitic soils: a micro-level investigation. Int. J. Geotech. Eng., 12(1): 46-52.

Vindula, S.K., Chavali, R.V.P., Reddy, P.H.P. and Srinivas, T. 2019. Ground granulated blast furnace slag to control alkali-induced swell in kaolinitic soils. Int. J. Geotech. Eng., 13(4): 377-384.

Wan, Y., Zhai, J. and Wang, A. 2021. Comparative study on electrode arrangement in electrokinetic remediation of contaminated soil. Nature Environ. Pollut. Technol., 20(1): 221-227.

Xiao, J. and Zhou, S. 2019. Effect of electrode materials on electrokinetic remediation of uranium-contaminated soil. IOP Conf. Ser. Earth Environ. Sci., 300(3): 032074.

Yi, X.U., Liang, X., Yingming, X.U., Xu, Q.I.N., Huang, Q., Lin, W.A.N.G. and Yuebing, S.U.N. 2017. Remediation of heavy metal-polluted agricultural soils using clay minerals: A review. Pedosphere, 27(2): 193-204.